RSC Advances

Conformation and adsorption transition on an attractive surface of a ring polymer in solution

Junfang Sheng[1] and Kaifu Luo[1, *]
[1] *CAS Key Laboratory of Soft Matter Chemistry,*
Department of Polymer Science and Engineering,
University of Science and Technology of China, Hefei, Anhui Province 230026, P. R. China

(Dated: November 15, 2014)

We investigate the effect of chain topology on conformation and adsorption transition on an attractive surface of a ring polymer in a dilute solution in a good solvent. Based on Flory theory, we find that the ratio of mean squared radii of gyration of a ring polymer and a linear chain of identical length is 0.574, which is in good agreement with the results from renormalization theory, previous simulations and experiments. Using three-dimensional Langevin dynamics simulations, we examine the adsorption transition of a flexible ring polymer chain with one bead grafted to a flat solid surface and the conformation of the adsorbed chain. Compared with the linear chain, the ring polymer has the same critical adsorption point (CAP). At the CAP, the crossover exponent of the number of adsorbed beads with chain length is about 0.50 for both ring and linear chains. At the CAP, ring polymers are adsorbed on the surface more than linear chains, which agrees with experiments. In addition, we further observe that, compared with linear chains, the adsorption of ring polymers is faster. Under strong attractions, we observe that the exponent of the adsorption time as a function of the chain length is $1 + \nu_{3D}$, where $\nu_{3D} = 0.588$ is the Flory exponent in three dimensions.

I. INTRODUCTION

The adsorption of polymer chain on a solid surface has been investigated for many years by theories [1–9], experiments [10–16] and simulations [2, 4, 17–28] due to its importance to practical applications, such as colloidal stabilization, lubrication and adhesion [29–31]. Understanding the process of the adsorption and the conformation of the adsorbed chain is also in favor of biological physics, such as proteins adsorbing on a membrane [32, 33].

The properties of a polymer solution are very different from the bulk when polymer interacts with an attractive surface. At the critical adsorption point (CAP), Polymer undergoes an adsorption transition from a three dimensional (3D) to a two-dimensional (2D) conformation. The adsorption transition can be explained as a second order phase transition at the CAP in the thermodynamic limit $N \to \infty$, with N being the chain length. At the CAP, the number of beads adsorbed on the surface at equilibrium, N_e, shows a scaling behavior with N, namely $N_e \sim N^{\phi}$ with ϕ being the crossover exponent.

For ideal chains, it has been known that $\phi = \frac{1}{2}$ [30]. The value of the crossover exponent ϕ in good solvent cases is fairly controversial. Based on scaling arguments, de Gennes [34] proposed $\phi = 1 - \nu$ with $\nu = 0.588$ being the Flory exponent in 3D [35], which would yield $\phi = 0.412$. However, it was pointed out [36] that this scaling relation underestimates ϕ, because the concentration profile of the monomer is assumed not to depend on the distance from the surface. Thus, this crossover exponent is more suitable for a penetrable surface than for the impenetrable one [37]. In contrast with this crossover exponent, lattice Monte Carlo (MC) simulation results [36, 38] gave $\phi = 0.58$, which is close to ν. Taking into account the proximal exponent [37], scaling theory can also give $\phi \approx \nu$. Using the pruned-enriched Rosenbluth method [39], Grassberger [40] has found $\phi = 0.48$, a little smaller than $\frac{1}{2}$.

By now, however, most of studies focus on adsorption of linear chains, where the structure of adsorbed polymer layers in solution is classically described in terms of loops, tails and trains, and the relative importance of loops and tails in an adsorbed polymer layer has also been addressed [43]. In contrast to linear chains, ring polymers do not have any tails and form adsorbed layers containing only loops and trains [41]. Thus, it is very important and meaningful to examine the adsorption of ring polymers. Experiments have shown that ring polymers under the same conditions are adsorbed more than the linear ones of the same molecular weight [42, 43]. In addition, lattice Monte Carlo (MC) simulation results have demonstrated that an adsorbed layer for a ring polymer begins to form at the larger adsorption transition temperature than that for a linear polymer chain [44].

It is clear that the adsorption transition for ring polymers is not well understood. In addition, it is also interesting to understand the difference of the adsorption between ring polymers and linear chains, which is induced by the topological constraint in ring polymers. The basic questions are the following: (a) Are the CAP and the crossover exponent for ring polymers the same as those for linear chains? (b) As to the linear chain or the ring polymer, which one is absorbed more and faster? (c) What's the ratio of N_e at the CAP for ring polymers and linear chains? To this end, we investigate the adsorption dynamics of a flexible ring polymer chain with

---

[*] Author to whom the correspondence should be addressed; Electronic address: `kluo@ustc.edu.cn`

one bead grafted to a flat solid surface and the conformation of the chain at the CAP using 3D Langevin dynamics simulations.

II. MODEL AND METHODS

In our numerical simulations, the polymer chains are modeled as bead-spring chains of Lennard-Jones (LJ) particles with the Finite Extension Nonlinear Elastic (FENE) potential. Excluded volume interaction between beads is modeled by a short range repulsive LJ potential: $U_{LJ}(r) = 4\varepsilon_0[(\frac{\sigma}{r})^{12} - (\frac{\sigma}{r})^{6}] + \varepsilon_0$ for $r \le 2^{1/6}\sigma$ and 0 for $r > 2^{1/6}\sigma$. Here, σ is the diameter of a bead, and ε_0 is the depth of the potential. The connectivity between neighboring beads is modeled as a FENE spring with $U_{FENE}(r) = -\frac{1}{2}kR_0^2\ln(1 - r^2/R_0^2)$, where r is the distance between consecutive beads, k is the spring constant and R_0 is the maximum allowed separation between connected beads.

We consider a schematic representation as shown in Fig. 1, where we give the chain conformation at absorption equilibrium for a ring polymer initially grafted to a smooth surface. The surface is formed by stationary particles of diameter σ, a series of beads closely packed at the $z = 0$ plane. During the adsorption process, the bead-wall particle interaction is modeled by an attractive LJ potential with a cutoff of 2.5σ and interaction energy ε. Although most of previous works use a strictly local interactions between the surface and the beads, here we use this more realistic potential [21].

In the Langevin dynamics simulation, each bead is subjected to conservative, frictional, and random forces, respectively, with [45] $m\ddot{\mathbf{r}}_i = -\nabla(U_{LJ}+U_{FENE})-\xi\mathbf{v}_i+\mathbf{F}_i^R$. Here m is the bead's mass, ξ is the friction coefficient, $\mathbf{v}_i$ is the bead's velocity, and $\mathbf{F}_i^R$ is the random force which satisfies the fluctuation-dissipation theorem. In the present work, the LJ parameters ε_0, σ, and m fix the system energy, length and mass units respectively, leading to the corresponding time scale $t_{LJ} = (m\sigma^2/\varepsilon_0)^{1/2}$ and force scale ε_0/σ, which are of the order of ps and pN, respectively. The dimensionless parameters in the model are chosen to be $R_0 = 1.5$, $k = 30$, $\xi = 0.7$ and $k_BT = 1.2$.

The Langevin equation is integrated in time by a method described by Ermak and Buckholz [46]. We initially fix the first bead of a linear chain but anyone of a ring chain at the center of a surface, while the remaining beads are under thermal collisions described by the Langevin thermostat to obtain an equilibrium conformation. During this relaxation process, the repulsive LJ potential is used for all particle pairs. After the equilibrium conformation of the chain is reached, we use the attractive LJ potential to model the bead-surface particle interaction during adsorption process. Once the number of beads adsorbed on the surface attains a balance, the time of the chain adsorption process, the number of the beads adsorbed on the surface at this time and a lot of conformational properties are all measured. In all of our simulations we did a number of runs with uncorrelated initial states. Typically, we average our data over 1000 independent runs.

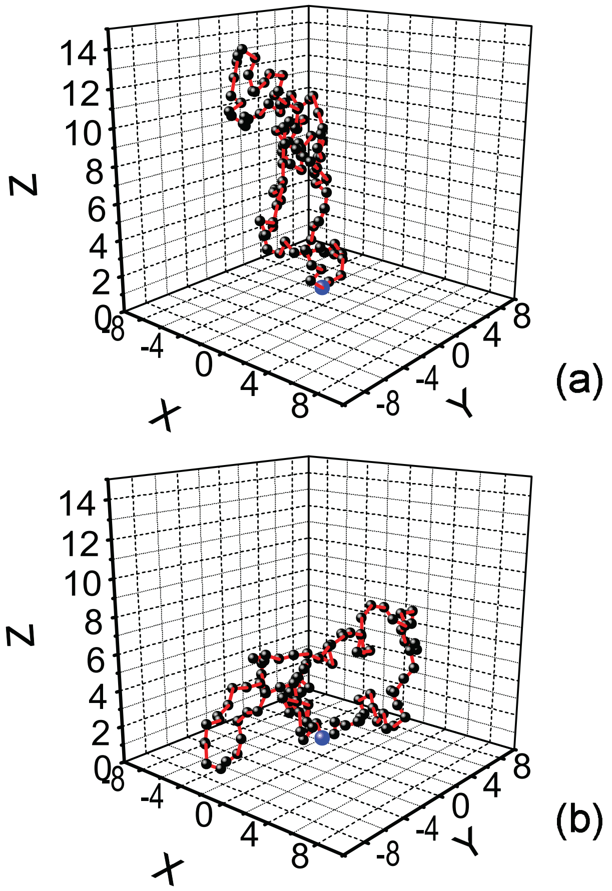

FIG. 1: A schematic representation of chain conformation at adsorption equilibrium for a ring polymer of length $N = 100$, which is initially grafted to the surface.

III. RESULTS AND DISCUSSION

A. Different conformational properties between ring and linear chains in dilute solution

Physically, it has been shown that the scaling behavior, $R_g \sim N^{\nu}$, should be the same for ring and linear chains, where R_g is the radius of gyration, N is the chain length and ν is the Flory exponent. To characterize the difference in chain conformation between the linear and the circular topologies, the G factor is used. The G factor is defined as $G = R_{g,r}^2/R_{g,l}^2$, where $R_{g,r}$ and $R_{g,l}$ are the radii of gyration for ring and linear chains, respectively. The value of G has been shown to be between 0.52 and 0.60 from renormalization theory [47], experiments [48], and simulations [49–52].

On the theoretical side, only renormalization theory is available. Here, we derive the G factor by using a relatively simple but understandable method. For a linear chain in good solvent conditions, the Flory theory [35] gives the chain free energy in unit of k_BT:

$$F = Av\frac{N^2}{R_g^3} + B\frac{R_g^2}{N\sigma^2}. \tag{1}$$

Here, A and B are constants, and v is an excluded volume for a monomer, depending on the solvent and the temperature. The first term is the excluded volume interactions and the second term is the elastic energy of the chain. For a ring polymer, we can consider it as two linear chains of identical length $\frac{N}{2}$ with their ends joined together to minimize the elastic energy. Then, we have

$$F = Av\frac{N^2}{R_g^3} + 2B\frac{R_g^2}{(\frac{N}{2})\sigma^2}. \tag{2}$$

To minimize the free energy $\frac{\partial F}{\partial R_g} = 0$, we obtain the size of the chain

$$R_{g,l} = (\frac{3Av}{2B})^{\frac{1}{5}} N^{\frac{3}{5}} \sigma^{\frac{2}{5}} \tag{3}$$

for linear chains and

$$R_{g,r} = (\frac{3Av}{8B})^{\frac{1}{5}} N^{\frac{3}{5}} \sigma^{\frac{2}{5}} \tag{4}$$

for ring polymers. Based on Eqs. (3) and (4), the radius of gyrations $R_{g,r}$ for ring polymers and $R_{g,l}$ for linear chains show the same scaling behavior and their ratio is

$$G = \frac{R_{g,r}^2}{R_{g,l}^2} = (\frac{1}{4})^{\frac{2}{5}} = 0.574 \tag{5}$$

Interestingly, our theoretical prediction of $G = 0.574$ based on Flory theory is in good agreement with $G = 0.568$ from renormalization theory [47], and is a little higher than the experimental value 0.52 [48]. There are many numerical values for the G factor using different simulation methods, and our prediction is between these values, namely 0.559 to 0.568 from Monte Carlo simulations [49, 50], 0.559 from Brownian dynamics simulations [51], and 0.607, 0.545, 0.553 from molecular dynamics, multiparticle collision dynamics and lattice Boltzmann simulations [52].

B. Adsorption transition

When using an attractive LJ potential, the criterion for adsorption is somewhat arbitrary [21, 53]. We define monomers with $z \leq 2.0$ as adsorbed, and thus monomers within the adsorption slab experience a z-dependent potential.

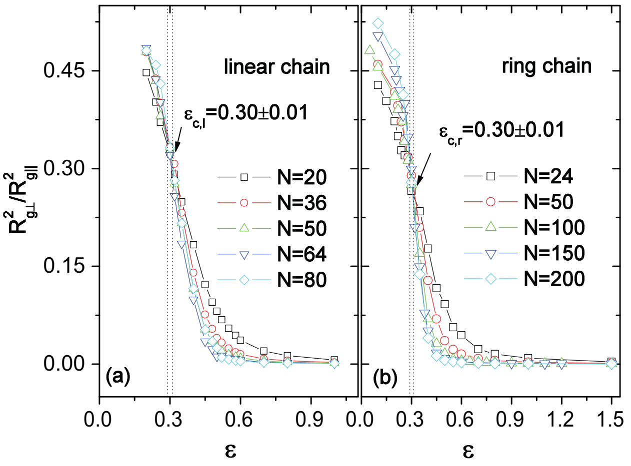

FIG. 2: The ratio of $R_{g\perp}^2$ to $R_{g\|}^2$ against ε for (a) the linear chain and (b) the ring polymer with different chain lengths. The $\varepsilon_c(\infty)$ is determined by the intersection of all curves which is at $\varepsilon = 0.30 \pm 0.01$ for both the linear chain and the ring chain.

1. *Critical adsorption point*

Here, we want to find the critical attractive strength $\varepsilon_c(N \to \infty)$ at the CAP. The radius of gyration, R_g, is an important parameter to describe the properties of adsorbed chains. In order to describe the components of R_g (radius of gyration in perpendicular direction $R_{g\perp}$ and in horizontal direction $R_{g\|}$), a parameter $\kappa = (\varepsilon - \varepsilon_c(\infty))/\varepsilon_c(\infty)$ is defined to measure the distance from the CAP and another variable $\eta \equiv \kappa N^\phi$ is also defined [36, 38]. Following references [36, 38], we have

$$R_{g\perp}(\eta) \sim \begin{cases} N^\nu \sigma, & \eta \leq 0 \\ \kappa^{-\nu/\phi}, & \eta \gg 0 \end{cases} \tag{6}$$

and

$$R_{g\|}(\eta) \sim \begin{cases} N^\nu \sigma, & \eta \leq 0 \\ \kappa^{(\nu_2-\nu)/\phi} N^{\nu_2}, & \eta \gg 0, \end{cases} \tag{7}$$

Where ν_2 is the Flory exponent in 2D. Descas *et al.* [38] have defined $r(\eta) \equiv R_{g\perp}(\eta)/R_{g\|}(\eta)$, which is used to find the CAP. At the CAP, the ratio $r(\eta)$ equals $r(0)$, which is a constant, independent of chain length N. So, from the intersect of the plots of $r(\eta)$ with ε for different N, one obtains $\varepsilon_c(\infty)$.

According to Eqs. (6) and (7), the ratio of $R_{g\perp}^2$ to $R_{g\|}^2$ is also independent of N at $\varepsilon_c(\infty)$. Fig. 2 shows $\varepsilon_c(\infty)$ at the CAP in the thermodynamic limit $N \to \infty$. We observe that the $\varepsilon_c(\infty)$ doesn't change with the chain topology and $\varepsilon_c(\infty) = 0.30 \pm 0.01$ for both the linear chain and the ring polymer.

To further confirm the observed behavior, we use another method to obtain the $\varepsilon_c(\infty)$ of the ring chain. We first define an order parameter $f_s = \frac{N_e}{N}$, which is the ratio of the final number of beads adsorbed on the surface

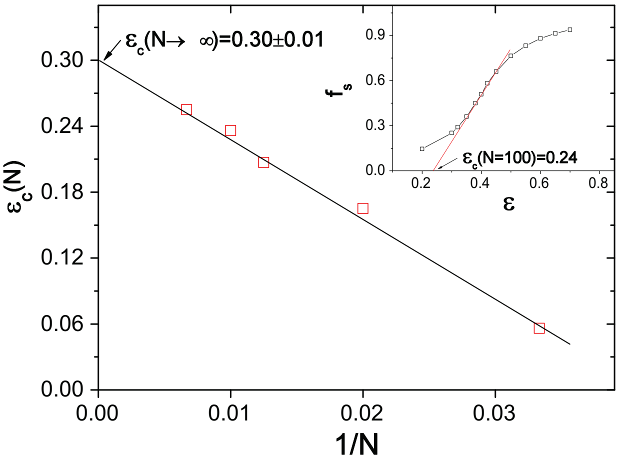

FIG. 3: The $\varepsilon_c(\infty)$ is extrapolated from the plot of $\varepsilon_c(N)$ versus $\frac{1}{N}$, which is about 0.30 ± 0.01. The order parameter $f_s = \frac{N_e}{N}$ is plotted against ε for a ring polymer of length N=100 as shown in the inset, the point where the tangent at the point of inflexion on the curve meets the abscissa is the CAP.

N_e to the chain length N. In the inset of Fig. 3, the order parameter f_s is plotted against ε for a chain of length $N = 100$. The point where the tangent at the point of inflexion on the curve meets the abscissa is the CAP for $N = 100$. Similarly, we get other values of $\varepsilon_c(N)$ for different chain lengths. In Fig. 3, based on the plot of $\varepsilon_c(N)$ versus $\frac{1}{N}$, we find $\varepsilon_c(\infty) = 0.30 \pm 0.01$, which is in good agreement with the value obtained from the first method.

In previous work by lattice MC simulation [44], it was found that an adsorbed layer for a ring polymer begins to form at the larger adsorption transition temperature than that for a linear polymer chain. This means the $\varepsilon_c(\infty)$ for the ring polymer is lower than that for the linear chain, which is different from our results here. The discrepancy may be from the lattice model used in previous work [44].

2. *Crossover exponent*

At the CAP, the number of finally adsorbed beads on the surface N_e shows a scaling behavior with the chain length N when N tends to infinity, $N_e \sim N^{\phi}$ with ϕ being the crossover exponent. Fig. 4 shows N_e as a function of the chain length N at the CAP for both ring and linear chains. We observe the scaling exponent $\phi = 0.53$ for the ring polymer and $\phi = 0.50$ for the linear chain, indicating that the crossover exponent almost doesn't change with the chain topology within the error range. These crossover exponents are in good agreement with previous theoretical [37] and numerical [21, 36, 38] results.

For different N, the values of N_e are always larger for ring polymers than those for linear chains of the same length. This is in good agreement with experimental results [42] and theoretical predictions [43] which show that ring polymers are adsorbed on a surface more than linear chains. Based on Fig. 4, we further find that the ratio of N_e for ring polymers to linear chains of identical chain lengths is about 1.25∼1.30. For ideal ring polymers and ideal linear chains, theory predicts the ratio to be 1.18 [54], which is a little smaller than our numerical result, indicating that this ratio slightly depends on the excluded volume effect.

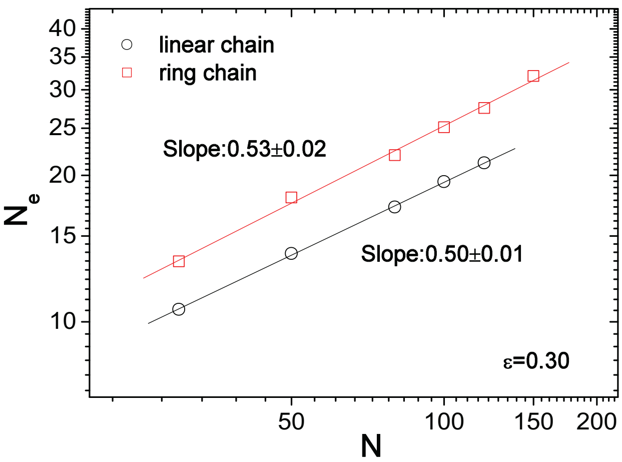

FIG. 4: Log-log plots of the final number of beads adsorbed on the surface N_e vs. N for the linear chain and the ring polymer at the CAP.

3. *Chain size at CAP*

Fig. 5 shows $R_{g\parallel}$ as a function of N at the CAP ($\varepsilon_c = 0.30$) after the adsorption equilibrium for both ring and linear chains. We observe the scaling exponents are 0.63 and 0.62 for the linear chain and the ring polymer, respectively, which are between the Flory exponent in 2D, $\nu_{2D} = 0.75$, and the Flory exponent in 3D, $\nu_{3D} = 0.588$ [35].

Although topological constraint in the ring chain does not lead to differences on the scaling relationship of $R_{g\parallel}$ with N, the value of $R_{g\parallel}$ of the ring chain is always smaller than that of the linear chain of the same N. Interestingly, their ratio is a constant, 0.73, which is close to the theoretical ratio value 0.76 for ring polymers and linear chains in dilute solution without adsorption.

C. Adsorption kinetics

1. *Number of adsorbed beads as a function of time*

Fig. 6 shows the average number of beads $n(t)$ adsorbed to the surface from different initial chain conformations as a function of the time for different attractive strengths ε. With increasing time, for both a ring polymer and a linear chain, $n(t)$ first increases until it

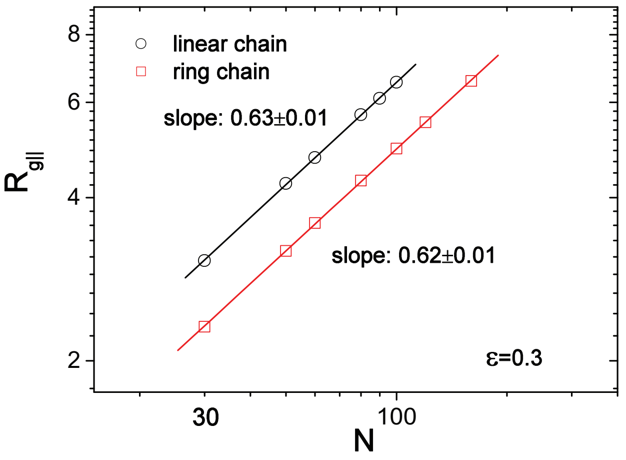

FIG. 5: Log-log plots of the gyration radius component $R_{g\|}$ vs. N at $\varepsilon = 0.30$ after the adsorption equilibrium for ring polymers and linear chains.

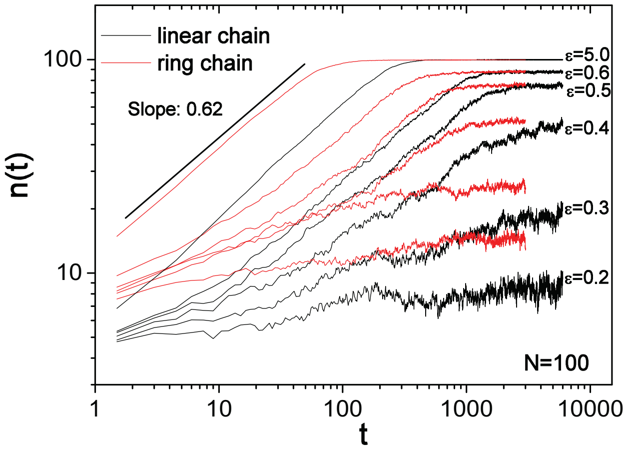

FIG. 6: Log-log plots of the number of the beads adsorbed to the plane as a function of the time for a ring polymer and a linear chain at different attractive strengths. The chain length is N=100 for both the ring polymer and the linear chain.

saturates to a constant, $N_e = n(t \to \infty)$, for different ε. Compared with the linear chain of the same chain length, adsorption of the ring polymer is faster to reach equilibrium. For a ring polymer and a linear chain, N_e is denoted by $N_{e,r}$ and $N_{e,l}$, respectively. With increasing ε in the range of $0.2 \leq \varepsilon \leq 5.0$, both $N_{e,r}$ and $N_{e,l}$ increase. In addition, $N_{e,r}$ and $N_{e,l}$ are the same at $\varepsilon \geq 0.4$, while $N_{e,r} \geq N_{e,l}$ at $\varepsilon \leq 0.30$. This indicates that, for very weak attractive potential, the fraction of beads at the surface is related to the loss of the entropy of the chain. The difference in conformational entropy loss on adsorption between rings and linear chains favors the adsorption of rings. Our results for weak adsorption are in agreement with experimental findings [42] and theoretical predictions [43] where ring polymers are adsorbed on a surface more than linear chains. For strong attractive potential $\varepsilon = 5$, we find $n(t) \sim t^{\beta}$, with $\beta \approx 0.62$.

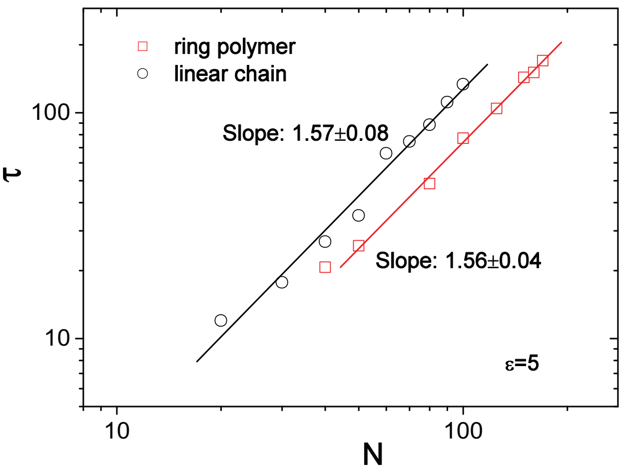

FIG. 7: Log-log plots of the time a chain to be adsorbed on the surface τ vs N for the linear chain and the ring chain at a strong attraction ε=5.

2. Adsorption time as a function of the chain length for strong attractions

For strong attractions, the adsorption can be considered to be irreversible and the bead attachment process obeys a simple "zipping" mechanism for linear chains [4, 55]. For ring polymers, we have checked the index of attached beads and observed the same mechanism. Fig. 7 shows the adsorption time τ as a function of the chain length N for both ring and linear chains at $\varepsilon = 5$. We observe $\tau \sim N^{\alpha}$, with the scaling exponent $\alpha = 1.57$ and 1.56 for the linear chain and the ring chain, respectively. These two exponents are very close to $1 + \nu_{3D}$, with $\nu_{3D} = 0.588$ being the Flory exponent in 3D. For linear chains, $\alpha = 1+\nu_{3D}$ has also been observed by both lattice [55–57] and off-lattice [4] Monte Carlo simulations.

Based on $n(t) \sim t^{\beta}$, when $n(t)$ is close to N, the adsorption time $\tau = t(N)$. Using $\beta \approx 0.62$ for $\varepsilon = 5$, we obtain $\tau \sim N^{\frac{1}{\beta}} = N^{1.61}$, which is in agreement with the above numerical results. This also indicates that $\beta = \frac{1}{1+\nu_{3D}}$ for strong attractive strengths. When adsorption is a sequential zipping process, the adsorption kinetics can be mapped exactly to polymer translocation dynamics under a transmembrane electric field [4], where the translocation time with chain length shows the same scaling behavior [58].

Another important result in Fig. 7 is that the adsorption for ring polymers is always faster than that for linear ones. We further find that the ratio of the adsorption times for the ring polymer and the linear chain of identical chain length is close to 0.57. The origin of this ratio comes from the ring topology.

IV. CONCLUSIONS

We investigate the effect of chain topology on conformation and adsorption transition on an attractive surface of a ring polymer in a dilute solution in a good solvent. Based on Flory theory, we find that the ratio of mean squared radii of gyration of a ring polymer and a linear chain of identical length is 0.574, which is in good agreement with the results from renormalization theory, previous simulations and experiments. Using three-dimensional Langevin dynamics simulations, we examine the adsorption transition of a flexible ring polymer chain with one bead grafted to a flat solid surface and the conformation of the adsorbed chain. Compared with the linear chain, the ring polymer has the same critical adsorption point (CAP). At the CAP, the crossover exponent of the number of adsorbed beads with chain length is about 0.50 for both ring and linear chains. At the CAP, ring polymers are adsorbed on the surface more than linear chains, which agrees with experiments. In addition, we further observe that, compared with linear chains, the adsorption of ring polymers is faster. Under strong attractions, we observe that the exponent of the adsorption time as a function of the chain length is $1 + \nu_{3D}$, where $\nu_{3D} = 0.588$ is the Flory exponent in three dimensions.

Acknowledgments

K.L. acknowledges support from the National Natural Science Foundation of China (Grants No. 21225421 No. 21174140 No. 21474099), the 973 Program of MOST (No. 2014CB845605), the Specialized Research Fund for the Doctoral Program of Higher Education (Grant No. 20103402110032), and the “ Hundred Talents Program ” of Chinese Academy of Science.

---

[1] P. G. de Gennes, *Macromolecules* **14**, 1637 (1981).
[2] H. Meirovitch, and S. Livne, *J Chem. Phys.* **88**, 4507 (1988).
[3] D. N. Theodorou, *Macromolecules* **21**, 1400 (1988).
[4] S. Bhattacharya, A. Milchev, V. G. Rostiashvili, A. Y. Grosberg, and T. A. Vilgis, *Phys. Rev. E.* **77**, 061603 (2008).
[5] B. O. Shaughnessy and D. Vavylonis, *Phys. Rev. Lett.* **90**, 056103-1 (2003).
[6] A. G. Cherstvy and R. G. Winkler, *Phys. Chem. Chem. Phys.* **13**, 11686 (2011).
[7] E. A. Di Marzio, C. M. Guttman, *Macromolecules* **20**, 1403 (1987).
[8] E. A. Di Marzio, *Macromolecules* **26**, 4613 (1993).
[9] E. Bouchaud, J. Vannimenus, *J.Phys. (France)* **49**, 2931 (1989).
[10] J. N. Israelachvili, and S. J. Kott, *J Chem. Phys.* **88**, 7162 (1988).
[11] J. P. Montfort, and G. Hadziioannou, *J Chem. Phys.* **88**, 7187 (1988).
[12] P. Frantz, and S. Granick, *Phys. Rev. Lett.* **66**, 899 (1991).
[13] E. Ercolini, F. Valle, J. Adamcik, G. Witz, R. Metzler, P. D. L. Rios, J. Roca, and G. Dietler, *Phys. Rev. Lett.* **98**, 058102 (2007).
[14] D. Horinek, A. Serr, M. Geisler, T. Pirzer, U. Slotta, S. Q. Lud, J. A. Garrido, T. Scheibel, T. Hugel, and R. R. Netz, *Proc. Natl. Acad. Sci.* **105**, 2842 (2008).
[15] F. Valle, M. Favre, P. D. L. Rios, A. Rosa, and G. Dietler, *Phys. Rev. Lett.* **95**, 158105 (2005).
[16] R. Yerushalmi-Rozen, B. J. Hostetter, L. J. Fetters, and J. Klein, *Macromolecules* **23**, 2984 (1990).
[17] P. Y. Lai, *Phys. Rev. E* **49**, 5420 (1994).
[18] P. Linse and N. Kallrot, *Macromolecules* **43**, 2054 (2010).
[19] Z. Benkova, B. Szefczyk, and M. N. D. S. Cordeiro, *Macromolecules* **44**, 3639 (2011).
[20] A. Sikorski, *Macromol. Theory Simul.* **10**, 38 (2001).
[21] S. Metzger, M. Muller, K. Binder, J. Baschnagel, *Macromol. Theory Simul.* **9**, 985 (2002).
[22] R. Hegger and P. Grassberger, *J. Phys. A* **27**, 4069 (1994).
[23] T. Vrbova and K. Prochazka, *J. Phys. A* **32**, 5469 (1999).
[24] E. J. J. Van Rensburg and A. R. Rechnitzer, *J. Phys. A* **37**, 4069 (2004).
[25] M. B. Luo, *J. Chem. Phys.* **128**, 044912 (2008).
[26] T. Chen, L. Wang, X. S. Lin, Y. Liu and H. J. Liang, *J. Chem. Phys.* **130**, 244905 (2009).
[27] L. Wang, T. Chen, X. S. Lin, Y. Liu and H. J. Liang, *J. Chem. Phys.* **131**, 244902 (2009).
[28] L. Hao, J. Y. Su, and H. X. Guo, *Chin. J. Polym. Sci.* **31**, 1066 (2013).
[29] A. K. Dolan and S. F. Edwards, *Proc. R. Soc. Lond.* **337**, 509 (1974); G.J. Fleer, J.M. Scheutjens, and M.A. Cohen Stuart, *Coll. and Surf.* **31**, 1 (1988).
[30] E. Eisenriegler, *Polymers near Surfaces*, World Scientific, Singapore, 1993.
[31] G. Fleer, M. Cohen-Stuart, J. Scheutjens, T. Cosgrove, B. Vincent, *Polymers at interfaces*, Chapman and Hall, London, 1993.
[32] A. F. Xie and S. Granick, *Nature Mater.* **1**, 129 (2002).
[33] B. Maier and J. O. Radler, *Phys. Rev. Lett.* **82**, 1911 (1999).
[34] P. G. de Gennes, *J. Phys. (France)* 37, 1445 (1976); *Macromolecules* 13, 1069 (1980).
[35] P. G. de Gennes, *Scaling Concepts in Polymer Physics* (Cornell University Press, Ithaca, NY, 1979).
[36] E. Eisenriegler, K. Kremer, K. Binder, *J. Chem. Phys.* 77, 6296 (1982).
[37] P. G. de Gennes, *J. Phys. Lett. (France)* 44, L241 (1983).
[38] R. Descas, J. U. Sommer, A. Blumen, *J Chem. Phys.* **120**, 8831 (2004).
[39] P. Grassberger, *Phys. Rev. E* 56, 3682 (1997).
[40] P. Grassberger, *J. Phys. A: Math. Gen.* 38, 323 (2005).
[41] J. A. Semlyen, *Cyclic Polymers*, 2nd ed. (Springer, Dordrecht, 2000).
[42] G. K. Stratouras, M. K. Kosmas, *Macromolecules* **25**, 3307 (1992); *ibid* **24**, 6754 (1991).
[43] B. Van Lent, J. Scheutjens, T. Cosgrove, *Macromolecules* **20**, 366 (1987).
[44] L. X. Zhang, A. Xia, Y. Xu, *Eur. Polym. J.* **36**, 847

(2000).
[45] M. P. Allen and D. J. Tildesley, *Computer Simulation of Liquids* (Oxford University, New York, 1987).
[46] D. L. Ermak and H. Buckholz, *J. Comput. Phys* **35**, 169 (1980).
[47] J. J. Prentis, *J Chem. Phys.* **76**, 1574 (1982).
[48] J. S. Higgins, K. Dodgson, J. A. Semlyen, *Polymer* **20**, 553 (1979); G. Voordouw, Z. Kam, N. Borochov, H. Eisenberg, *Biophys. Chem.* **8**, 171 (1978)
[49] W. Bruns and J. Naghizadeh, *J Chem. Phys.* **65**, 747 (1976).
[50] Y. D. Chen, *J Chem. Phys.* **74**, 2304 (1981); *ibid* **75**, 2447 (1981).
[51] N. Kanaeda and T. Deguchi, *J. Phys. A: Math. Theor.* **41**, 145004 (2008).
[52] G. A. Hegde, J. F. Chang, Y. L. Chen,and R. Khare, *J. Chem. Phys.* **135**, 184901 (2011).
[53] Y. Yoshinaga, E. Kats, and A. Halprin, *Macromolecules* **41**, 7744 (2008).
[54] M. K. Kosmas, *Macromolecules* **23**, 2061 (1990).
[55] R. Descas, J.-U. Sommer, A. Blumen, *J Chem. Phys.* **124**, 094701 (2006).
[56] J. S. Shaffer, *Macromolecules* **27**, 2987 (1994).
[57] A. L. Ponomarev, T. D. Sewell, and C. J. Durning, *Macromolecules* **33**, 2662 (2000).
[58] K. Luo, T. Ala-Nissila, S. C. Ying, and R. Metzler, *EPL* **88**, 68006 (2009).

TOC

Ring polymers have the same critical adsorption point and crossover exponent as linear chains.